Metallomics, 0, 2024, mfae048
https://doi.org/10.1093/mtomcs/mfae048
Advance access publication date: 23 October 2024
Paper

Nitrogen fertilizers activate siderophore production by the common scab causative agent *Streptomyces scabiei*

Nudzejma Stulanovic[1], Yasmine Kerdel[1], Loïc Belde[1], Lucas Rezende[2], Benoit Deflandre[1], Pierre Burguet[3], Romane Denoel[1], Déborah Tellatin[1], Augustin Rigolet[4], Marc Hanikenne[5], Loïc Quinton[3], Marc Ongena[4], Sébastien Rigali[1,*]

[1]InBioS—Center for Protein Engineering, Institut de Chimie, University of Liège, B-4000 Liège, Belgium, [2]Hedera-22, Boulevard du Rectorat 27b, B-4000 Liège, Belgium, [3]Department of Chemistry, University of Liège, B-4000 Liège, Belgium, [4]Microbial Processes and Interactions, TERRA Teaching and Research Center, BioEcoAgro, Joint Research Unit/UMR Transfrontalière 1158, University of Liège—Gembloux Agro-Bio Tech, Gembloux, Belgiums and [5]InBioS—PhytoSystems, Translational Plant Biology, University of Liège, B-4000 Liège, Belgium
*Corresponding author: E-mail: srigali@uliege.be

Abstract

Streptomyces scabiei is the causative agent of common scab on root and tuber crops. Life in the soil imposes intense competition between soil-dwelling microorganisms, and we evaluated here the antimicrobial properties of *S. scabiei*. Under laboratory culture conditions, increasing peptone levels correlated with increased growth inhibitory properties of *S. scabiei*. Comparative metabolomics showed that production of *S. scabiei* siderophores (desferrioxamines, pyochelin, scabichelin, and turgichelin) increased with the quantity of peptone, thereby suggesting that they participate in growth inhibition. Mass spectrometry imaging further confirmed that the zones of secreted siderophores and growth inhibition coincided. Moreover, either the repression of siderophore production or the neutralization of their iron-chelating activity led to increased microbial growth. Replacement of peptone by natural nitrogen sources regularly used as fertilizers such as ammonium nitrate, ammonium sulfate, sodium nitrate, and urea also triggered siderophore production in *S. scabiei*. The observed effect is not mediated by alkalinization of the medium as increasing the pH without providing additional nitrogen sources did not induce siderophore production. The nitrogen-induced siderophore production also inhibited the growth of important plant pathogens. Overall, our work suggests that not only the iron availability but also the nitrogen fertilizer sources could significantly impact the competition for iron between crop-colonizing microorganisms.

Keywords: siderophore production control; iron piracy; nitrogen fertilizers; common scab; plant pathogen, potato disease

Graphical abstract

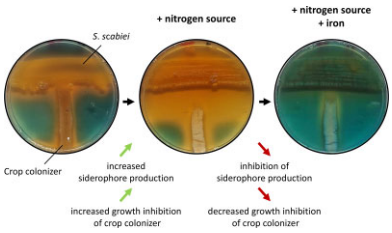

Introduction

Several characteristics and strategies enable microorganisms to thrive in the rhizosphere [1]. Nutritional versatility is certainly one of the main assets, as is the ability to respond appropriately to regularly fluctuating biotic and physicochemical factors. Filament-forming bacteria and fungi lack the motility needed to reach nutrient-rich zones or escape adverse conditions. However, they compensate with larger genomes encoding enzymes needed to feed on the most diverse carbon sources, as well as numerous genes for the biosynthesis of specialized molecules with a wide range of biological activities [2–6]. Among the molecules of secondary (specialized) metabolism, those involved in antagonistic interactions, such as antimicrobial agents, enable these non-motile micro-organisms to secure a feeding zone where development is authorized only to members of the microbial community possessing the resistance mechanisms. In this context, siderophores are of particular interest, as they contribute both to satisfying nutritional requirements by supplying the iron needed for basic biological functions, and this sequestration of environmental iron also strongly impacts antagonistic interactions due to the deprivation of this essential element [7–9].

Rhizosphere microorganisms that have developed a pathogenic lifestyle must additionally possess the genetic material needed to colonize their host [10]. This includes specialized metabolites with phytotoxic activity, but also metabolites that participate in the defense strategy against the host response. *Streptomyces scabiei* (synon. *Streptomyces scabies*) and closely related pathogenic *Streptomyces* species are filamentous Gram-positive bacteria responsible for the common scab disease of root and tuber

Received: August 19, 2024. **Accepted:** October 22, 2024
© The Author(s) 2024. Published by Oxford University Press. All rights reserved. For permissions, please e-mail: journals.permissions@oup.com

crops. In general, the virulence of the strain correlates with the production level of thaxtomin phytotoxins, although notable exceptions were recently reported suggesting a major contribution of other virulence genes. Besides thaxtomins, other specialized metabolites are part of the 'virulome' induced by the elicitors of the pathogenic lifestyle including other phytotoxins, and siderophores among other biomolecules for which their specific role in host colonization is still unclear [11, 12].

Although numerous studies have been devoted to characterizing the metabolism of *S. scabiei* associated with the interaction with its plant hosts [11, 13], very few studies have focused on molecules potentially involved in antagonistic interactions with other microorganisms. Microbe–microbe interactions are expected to occur with other saprophytic microorganisms of the rhizosphere, but also with the microorganisms recruited by the host to guarantee its self-defense. In addition, as common scab neither kills the plant nor alters the biological functions of the infected organs, it is plausible that, under certain conditions, *S. scabiei* could play a protective role for its hosts against much more destructive pathogens. Earlier work reported antifungal and antioomycete activities for strain PK-A41 of *S. scabiei* [14], and genomic and metabolomic studies confirmed its capability to produce concanamycin derivatives active against bacteria, fungi, and oomycetes [11, 12].

In this work, we investigated under which culture conditions *S. scabiei* 87-22 displays antimicrobial activities against a series of microorganisms including eminent plant pathogens. Under certain laboratory culture conditions siderophore-mediated competition was observed, and the search for the nutrient elicitor revealed that this process was activated by nitrogen fertilizers commonly used as soil improvers. A first version including most of the results of this work was initially published in *Metallomics* (https://doi.org/10.1093/mtomcs/mfae021). This publication was retracted at our own request after we realized that most of our experiments had been carried out with a strain other than the one referenced in the manuscript. Thus, regardless of the rigor of the data, the context of the work and the objectives were incorrect.

Materials and methods

Strain maintenance and cultivation media

Spore stocks of *S. scabiei* 87-22 [15] grown on instant potato mash (IPM) agar plates were prepared as described in *Practical Streptomyces Genetics* [16] stored at −80°C or −20°C. *Streptomyces scabiei* cultivation media used were (for 1 liter) International Streptomyces Project (ISP) media (No. 1–7) prepared according to Shirling and Gottlieb [17]; Glucose Yeast extract Malt extract [glucose 4 g, yeast extract 4 g, malt extract 10 g, $CaCO_3$ 2 g, and Bacto Agar (BD Difco™) 20 g, and pH adjusted to 7.3 ± 0.2]; Yeast extract-Malt extract (YM) medium [yeast extract (VWR™) 3 g, Bacto™ Malt Extract (Gibco™) 3 g, D(+)-glucose monohydrate (Carl Roth®) 10 g, bacteriological peptone (Condalab) 5 g, and Bacto Agar (BD Difco™) 20 g]; soy flour mannitol (SFM) media were prepared according to the protocol described; IPM medium consists of 50 g of Maggi Mousline (Nestlé®) powder and 12 g of Bacto Agar (BD Difco™) dissolved in tap water; CD (Czapek-Dox) medium [sucrose 30 g, $NaNO_3$ 2 g, K_2HPO_4 1 g, $MgSO_4$ 0.5 g, KCl 0.5 g, $FeSO_4$ 0.01 g, and 15 g of Bacto Agar (BD Difco™) 20 g, and pH adjusted to 7.3 ± 0.2]; lysogeny broth [LB25 g/l and bacteriological agar (VWR™) 20 g]; V8 agar medium was prepared by dissolving 15 g of Bacto Agar (BD Difco™) and 3 g of calcium carbonate in 200 ml of V8® vegetable juice, which was then mixed with 800 ml of distilled water; and the pH was adjusted to 7.2. Rye solution (rye grain from Vajra) was prepared according to Caten and Jinks [18].

Precultures of *Penicillium restrictum* NS1 (MUCL 58442), *Alternaria solani* (Ellis & Martin) Sorauer, *Gibberella zeae* (Centre d'Ingénierie des Protéines collection strain), and *Fusarium culmorum* (MUCL42823) were prepared as follows: a 40% glycerol mycelium stock preserved at −80°C was used to inoculate Potato Dextrose Agar (PDA) plates and incubated 3 days at 28°C; a V8 agar plate was inoculated with a mycelium plug of *Pythium ultimum* (DSM 62987). After 5 days at room temperature, new mycelium-rich plugs were taken from this plate and used to further assays.

Antimicrobial assays

Cross-streak assays

The growth inhibition activity against *P. restrictum* NS1, *A. solani*, *F. culmorum*, and *G. zeae* was first evaluated by cross-streak assays on solid media as previously described [19, 20]. For *S. scabiei* 87-22, a 4 µl of spore suspension (5.10^6 spores/ml) was used to inoculate a single streak in the upper part of the Petri dish and plates were incubated at 28°C for 4 days. Fungal mycelium suspension (OD_{625} at 0.1 in water for mycelium scrapped from a 3-day culture at 28°C on PDA) was inoculated with a cotton swab as a single streak perpendicular to the band of *Streptomyces*. *Pythium ultimum* was inoculated by transferring a mycelium-rich plug from a V8 agar plate to plates that had previously been inoculated with *S. scabiei* for subsequent tests.

Assessment of fungal growth on liquid media

The assessment of *P. restrictum* NS1 growth in liquid media was performed in 24-multiwell plates (Greiner 24 Flat BoZom Transparent Polystyrene) where each well contained 100 μl of concentrated (10×) YM medium (in order to guarantee similar amount of nutrients), 900 and 500 μl of the *S. scabiei* culture extract for 10% and 50% dilutions, respectively, and the total volume was adjusted to 1 ml with distilled water; 5 µl of *P. restrictum* NS1 spores (OD_{625} = 0.08–0.12) was used for inoculation and its growth was evaluated after 3 days of incubation at 28°C using Tecan Infinite® 200 PRO Plate Reader. The feature parameters were set on multiple reads per well (11×11) with a 0-μm border. The number of flashes was set to 25, bandwidth to 9 nm, and settle time to 0 ms. The measurements were carried out at a wavelength of 620 nm. The same experiment but with pure desferrioxamine B (DFOB; deferoxamine mesylate, MerckMilipore®) followed a similar protocol; specifically, wells containing 500 μl of concentrated (2×) rye solution were supplemented with 500 μl of either DFOB or ferrioxamine B (DFOB complexed to Fe^{3+}, DFOB solution with equimolar quantities of $FeCl_3$).

Quantification of siderophore production by the chrome azurol S colorimetric assay

Siderophore production was monitored by the colorimetric chrome azurol S (CAS) assay [21]. The methodology is based on the high affinity of siderophores for iron, which will capture the iron from an iron–dye complex, and the iron-free dye changes in color from blue to orange. Chrome azurol S was prepared as described by Schwyn and Neilands [21]; 60.5 mg of CAS (Acros Organics™) was dissolved in 50 ml of deionized water and mixed with 10 ml of an iron (III) solution (1 mmol/l $FeCl_3 \cdot 6H_2O$ and 10 mmol/l HCl), and 72.9 mg of hexadecyltrimethylammonium bromide (Acros Organics™) dissolved in 40 ml of deionized water was finally added before autoclaving. Rough estimation

of siderophore production was usually performed by CAS agar diffusion (CASAD) assays [22] by pouring the culture extract into wells dug into plates with solid CAS–agar media (CAS mixed with a 2% agarose solution in a 1:5 ratio) as performed previously [23, 24]. Alternatively, the CAS–agar solution was directly poured onto the bacteria grown on solid plates.

Semiquantification of siderophores was performed by mixing 100 µl of the liquid CAS solution with 100 µl of the culture extract. After 20 min of incubation, the absorbance of each sample was recorded at either at 630 nm (loss of the blue color) or at 480 nm (appearance of the yellow/orange color). Siderophore production was calculated using following formula: siderophore production (% siderophore unit psu) = ((Ar—As) × 100)/Ar, where Ar is the absorbance of the reference (CAS solution and un-inoculated medium), and As is the absorbance of the sample (CAS solution and mycelium-free supernatant of sample) [25].

Ultra-performance liquid chromatography–high-resolution mass spectrometry

Plates with YM media containing 0, 2.5, 5, 10, and 25 g/l of peptone were inoculated with 10^7 spores/ml of *S. scabiei* and incubated for 4 days at 28°C. Extraction of metabolites was done using the freeze-thaw method, which includes freezing the plates at −20°C and slow thawing at 37°C followed by collecting the thawed liquid. Prior to mass spectrometry (MS) analysis, all samples were filtered on 0.22 µm. The ultra-performance liquid chromatography–high-resolution mass spectrometry (UPLC–HRMS) analyses were performed on a Waters ACQUITY Ultra Performance LC system equipped with a Waters Synapt XS Q-TOF. A 5.0 μl of sample solution was injected for each run. Chromatographic separation was performed with a flow of 0.5 ml/min, at 40°C, using the 1.7-µm ACQUITY UPLC BEH C18 Column (2.1 mm × 50 mm dimension, 130 Å pores). The mobile phase consisted of water (containing 0.1% formic acid—solvent A) and acetonitrile (ACN; containing 0.1% formic acid—solvent B). The elution gradient was 0–1 min, 1% B; 1.0–15.0 min, 1%–80% B; 15.0–25.0 min, 80%–100% B; 25.0–28.0 min, 100% B; 28.0–28.5 min, 100.0%–1.0% B; and 28.5–30.0 min, 1.0% B. Mass spectrometry analyses were performed on positive electrospray polarity with a source temperature of 150°C. The capillary and cone voltage were set at 0.5 kV and 70 V, respectively. An High Definition Mass Spectrometry Elevated Energy continuum function in resolution mode with an extended dynamic range, a scan range of 50–2000 *m/z*, and a scan time of 0.15 s was used. For the high-energy (MS2) data collection, a collision energy ramp from 20 to 70 V was set for the transfer cell. All analyses were acquired using a leucine enkephalin solution (100 ng/ml in H_2O/ACN 50:50) as the lockmass.

Progenesis QI was used for liquid chromatography–mass spectrometry (LC–MS) data analysis, including lockspray correction, alignment, peak picking, adduct deconvolution, and annotation. Lockspray correction was performed based on the calculated monoisotopic mass of the $M+H^+$ ion of leucine enkephalin (556.2766). An abundance threshold of 500 was used to filter out background features. Similarly, data from control experiments with noninoculated media were used in order to filter out irrelevant features. The following adducts were considered for adduct deconvolution: $[M+H]^+$, $[M+Na]^+$, $[M+K]^+$, $[M–H_2O+H]^+$, $[M–H_2O+H]^+$, $[2M+H]^+$, and $[2M+Na]^+$. Progenesis MetaScope plug-in was used in the metabolite identification step. For that, genome mining information was used to generate an .sdf file containing a database of predicted metabolites, which was then used for annotation with a 10-ppm error tolerance (Supplementary File S1). A feature table was exported on csv format and included information such as neutral mass, *m/z*, adducts, retention time, collision cross section, and normalized abundance (supplementary material available on request). An annotation table containing compound description, and annotation quality metrics calculated by Progenesis QI (mass error, isotope similarity, and fragmentation score), was also generated and exported on csv format (Supplementary File S2). In line with our internal quality control analyses and with literature data, annotations with a fragmentation score <20 were not accepted [26, 27].

Sample preparation for mass spectrometry imaging

Microbial streaks on the solid medium were cut directly from the agar plate and transferred to a microscope slide (VWR, USA), previously covered with a double-sided conductive copper tape (3M). Before applying the matrix, the slides were dried at 40°C for 2 h. For mass spectrometry imaging (MSI), an α-Cyano-4-hydroxycinnamic acid matrix solution was prepared at 5 mg/ml in 80/20 ACN/water doped with 0.1% formic acid. Then we used a matrix sprayer (SunChrom, Friedrichsdorf, Germany), where air pressure was set to 2.5 bar, and we sprayed four cycles of 10 layers of matrix onto the slides. The first layer was sprayed at a flow rate of 10 μl/min. The flow rate for the first layer was set to 10 µl/min; second layer, 20 µl/min; third, 30 µl/min; fourth, 40 µl/min; and fifth to seventh, 60 µl/min. The track speed and track spacing were set to 800 mm/min and 2 mm, respectively.

Fourier transform ion cyclotron resonance mass spectrometry and data analysis

MSI data of the samples were acquired on Solarix XR 9.4T (Bruker Daltonics, Bremen, Germany) with a file size of 2M (Full Width at Half Maximum ± 300 000 at 400 *m/z*). The mass spectrometer was systematically mass calibrated from 150 to 1600 *m/z* before each analysis with a red phosphorus solution in pure acetone spotted directly onto the slides covered with a double-sided conductive copper tape to reach a mass accuracy better than 0.2 ppm. FlexImaging v5 (Bruker Daltonics, Bremen, Germany) software was used for Matrix-Assisted Laser Desorption/Ionization MS imaging acquisition, with a pixel step size for the surface raster set to 200 μm. For each mass spectrum, one scan of 20 laser shots was performed at a repetition rate of 200 Hz. The laser power was set to 14% and the beam focus was set to 'small'. Finally, raw MSI data were imported into SCiLS Lab 2016b software to construct MS image to visualize mass [28].

Results and discussion

Peptone activates the antifungal activity of *S. scabiei*

The antifungal activities of *S. scabiei* inoculated on 10 different solid media were assessed through the cross-streak method. Full growth inhibition of *P. restrictum* NS1 was observed in ISP1, ISP6, LB, Tryptic Soy Agar, and Mueller-Hinton Agar media (Fig. 1A), suggesting the production of toxic volatile compounds (Supplementary File S3). In contrast, no inhibition was observed in ISP7, IPM, and SFM media. On the YM medium and to a lesser extent on ISP2, growth inhibition was observed with levels ranging between these extreme cases (full and no

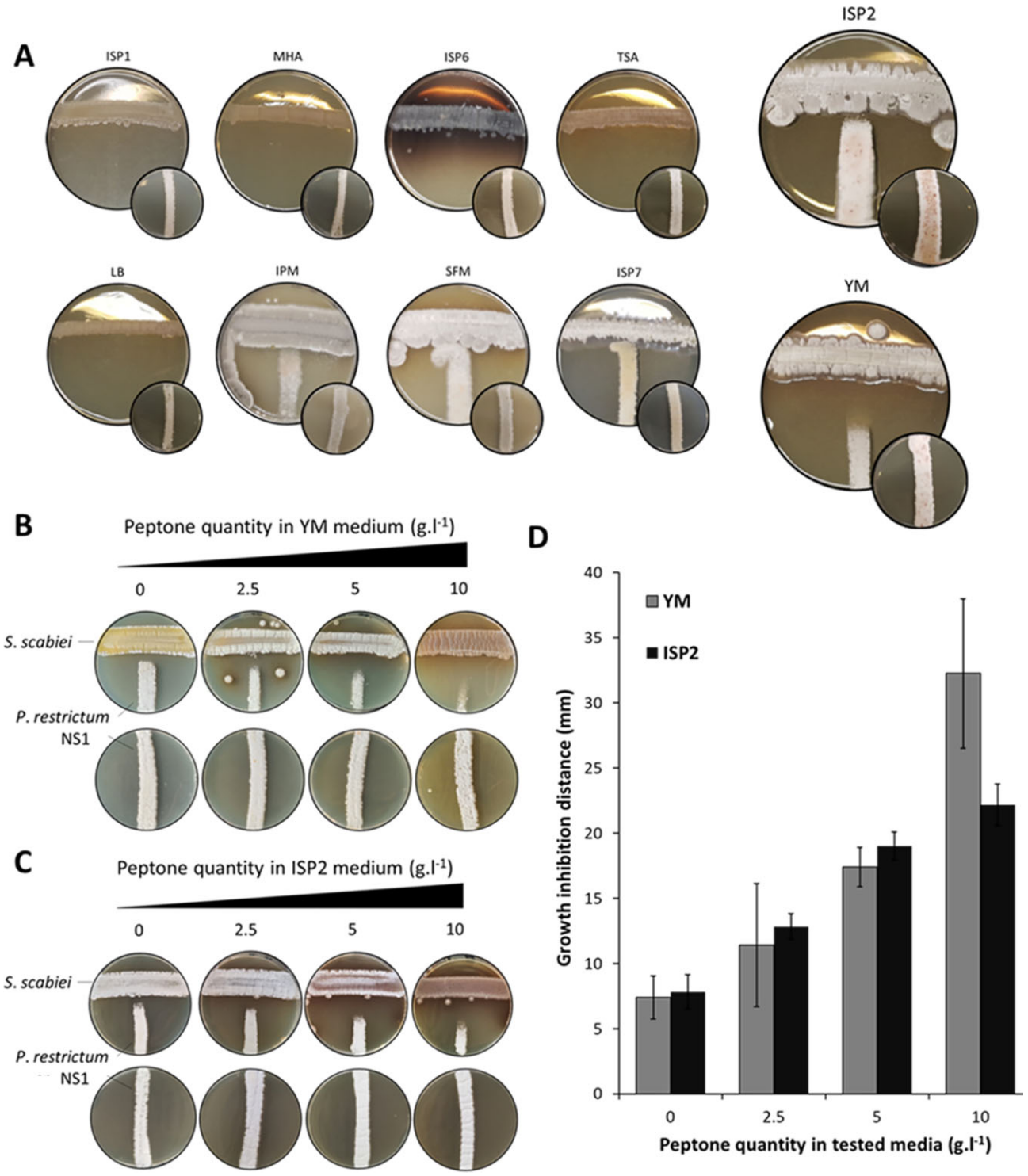

Figure 1. Peptone activates the antifungal activity of *S. scabiei*. (**A**) Cross-streak assays with *S. scabiei* inoculated 4 days prior to *P. restrictum* NS1. Insets in the lower right part of each cross-streaked plate: growth of *P. restrictum* NS1 on the control plate in the absence of *S. scabiei*. Cross-streaks showing the correlation between the antifungal activity of *S. scabiei* according to the peptone quantity (0–10 g/l) in YM (**B**) and ISP2 (**C**) media. **D.** Quantification of the growth inhibition of *P. restrictum* NS1 by *S. scabiei* according to the amount of peptone in YM and ISP2 media. Error bars represent standard deviations expressing the variability among four biological replicates for each condition.

inhibition), suggesting the production of agar diffusible antifungal molecules (Fig. 1A). Both media have a very similar nutrient composition with yeast extract (4 $g{\cdot}l^{-1}$ vs 3 $g{\cdot}l^{-1}$), malt extract (10 $g{\cdot}l^{-1}$ vs 3 $g{\cdot}l^{-1}$), and glucose (4 $g{\cdot}l^{-1}$ vs 10 $g{\cdot}l^{-1}$) for ISP2 and YM, respectively. The main difference is the addition of peptone (5 $g{\cdot}l^{-1}$) in the YM medium. We prepared both media with different amounts of peptone to assess how the oligopeptides and/or amino acids present in peptone affect the production of compounds inhibiting the growth of *P. restrictum* NS1. Increasing the amount of peptone in the YM medium correlates with

increased growth inhibition (Fig. 1B). The inhibition observed without peptone is ~7 mm and increases up to 32 mm on average at 10 $g \cdot l^{-1}$ of peptone, representing a ~4.5-fold increase of the inhibitory effect (Fig. 1D). Moreover, including peptone in the ISP2 medium also resulted in increased growth inhibition to levels similar to those observed in the YM medium (Fig. 1C and D). We therefore conclude that oligopeptides and/or amino acids present in peptone serve as elicitors for the production by *S. scabiei* of agar-diffusible antifungal compound(s).

Peptone-mediated induction of siderophore production inhibits fungal growth

Full extracts of *S. scabiei* grown on YM without peptone or with increasing quantities of peptone (2.5, 5, and 10 $g \cdot l^{-1}$) were analyzed by comparative metabolomics to identify compounds which secretion levels correlate with the increasing quantity of peptone in the cultivation medium. Figure 2A displays the absolute abundance of ions with *m/z* associated with known specialized metabolites of *S. scabiei* detected in our experimental conditions.

Based on filter parameters and quality control criteria (see the 'Materials and methods' section), 23 compounds were unambiguously identified by UPLC–HRMS, namely desferrioxamine, pyochelin, turgichelin, and scabichelin siderophores, the autoregulative spore germination inhibitors germicidins, the thaxtomin phytotoxins, the volatile bicyclic terpene geosmin, the macrocyclic peptide bottromycin antibiotics active against Gram-positive bacteria, and the 2,5-diketopiperazine cyclo(L-Pro-L-Val) antibiotic also active against Gram-positive bacteria. In terms of absolute ion abundance (the area of the chromatographic peak), desferrioxamine E (DFOE) and DFOB are by far the most abundant compounds identified (Fig. 2A). Interestingly, the relative abundance of DFOE and DFOB displays the sought-after production profile; i.e. their production increases with the quantity of peptone added to the cultivation medium. The same positive correlation between the quantity of peptone and the metabolite abundance is also observed for the 13 other forms of desferrioxamines identified, as well as for all other siderophores, namely pyochelin, scabichelin, and turgichelin (Fig. 2A). Siderophore detection using the CAS assay further confirmed the strong correlation between the production of iron-chelating metabolites and the concentration of peptone in the YM medium (Fig. 2B). Bottromycin A2 and germicidins were the only nonsiderophore metabolites that also displayed substantially increased abundance according to the quantity of peptone in the YM medium. Instead, the relative abundance of thaxtomin phytotoxins decreases with the quantity of peptone, whereas geosmin production levels remained rather similar under the four culture conditions tested. Importantly, as the ions corresponding to concanamycins were not detected in our samples, they are unlikely to be the metabolites responsible for the observed increasing antifungal activity of *S. scabiei*. Instead, siderophore production is highly triggered by the quantity of peptone in the YM medium, thereby being the best candidate metabolites for a role in the observed increased antifungal activity.

As siderophore production is naturally controlled by iron availability, we increased the concentration of $FeCl_3$ in the YM medium and assessed its impact on both siderophore production and the global antifungal activity of *S. scabiei*; 100 µM of $FeCl_3$ is sufficient to repress siderophore production when *S. scabiei* 87-22 is grown on the YM medium containing the amount of peptone that best stimulates siderophore production (5 and 10 $g \cdot l^{-1}$, see Fig. 2B), as deduced from the loss of the orange halo in the CASAD assays (Fig. 3A). The addition of iron in the YM medium containing peptone also results in a reduced inhibition zone of *P. restrictum* NS1 (Fig. 3B). At 10 µM of $FeCl_3$, the reduction of the growth inhibition is estimated to 40% and 70% in YM either containing 5 or 10 $g \cdot l^{-1}$ of peptone, respectively (Fig. 3C). Increasing the concentration of $FeCl_3$ up to 100 µM still slightly reduces the inhibition but without ever observing its total loss, suggesting the production of another compound with antifungal activity under the culture conditions tested (Fig. 3C).

Similar cross-streak assays were conducted against four plant pathogens, namely *A. solani*, *F. culmorum*, *G. zeae*, and *P. ultimum*. The results, as shown in Fig. 4, indicated that the growth of *A. solani*, *G. zeae*, and *P. ultimum* was significantly reduced with the addition of the quantity of peptone that best enhances siderophore synthesis. However, the addition of peptone did not reduce the growth of *F. culmorum*, possibly due to the ability of this strain to import some of the ferri-siderophore secreted by *S. scabiei*. The contribution of the siderophore-mediated growth inhibition induced by the addition of peptone was confirmed by the loss of growth inhibition upon addition of 100 µM of $FeCl_3$. The growth restoration effect of $FeCl_3$ supply was more pronounced in cross-streak assays with 10 g of peptone, which further confirms the significant contribution of siderophores at impairing the development of the tested microorganisms. Yet, the addition of iron did not fully restore the growth of tested microorganisms, again suggesting the presence of other compounds with antagonizing activity.

Additionally, the peptone-induced production of siderophores was assessed by MSI coupled to Fourier transform ion cyclotron resonance technology (Fig. 5A). The zone of growth inhibition in cross-streak assays was directly sampled from the agar plate and treated by MSI for high-resolution mapping of ions. As control, we also collected MSI data for each culture condition without microorganism inoculation. As shown in Fig. 5A, ions corresponding to DFOE and DFOB and scabichelin siderophores are only detected in the YM medium containing peptone, and the addition of 10 µM of $FeCl_3$ in the medium represses the production of both types of siderophores. MSI also revealed that the zones of siderophore production by *S. scabiei* correspond to the zone of growth inhibition of *P. restrictum* NS1, further supporting their causative role in antifungal activity. CAS agar overlay on cross-streak assays confirmed that the addition of 10 µM of $FeCl_3$ in the YM medium containing peptone resulted in both reduced siderophore production and a decrease of the antifungal activity (Fig. 5B).

Siderophores inhibit growth by iron exploitative competition

If the growth inhibition of *P. restrictum* NS1 is a consequence of the sequestration of iron by the siderophores produced by *S. scabiei*, the observed antagonism between both microorganisms should be attenuated by adding iron to the *S. scabiei* culture extracts. Indeed, the addition of excess iron should saturate uncomplexed siderophores thereby allowing *P. restrictum* NS1 to acquire iron from the cultivation medium. Figure 6A reveals that concentrations of $FeCl_3$ ranging from 100 to 500 µM decrease the iron chelation signal in CAS assays with total loss of the orange halo revealing the iron-chelating activity of the *S. scabiei* extracts at 500 µM.

The same *S. scabiei* culture extracts with or without $FeCl_3$ concentrations of 100, 200, and 500 µM were used to assess the growth inhibition of *P. restrictum* NS1. As shown in Fig. 6B, the addition of iron in the most concentrated culture extract (10% dilution) of *S. scabiei* could moderately restore the growth of *P.*

A

	Compound [adduct]	Mass (Da)	ppm	peptone (g.l^{-1}) in YM medium: 0	2.5	5	10
1	**desferrioxamine E** $[M+H]^+$, $[M+Na]^+$	600.3482	-4.94	22	1445	30376	436883
2	**desferrioxamine B** $[M+H]^+$	560.3533	-3.07	0	375	40385	327242
3	**germicidin B** $[M+H]^+$	182.0942	-3.15	395	3105	8411	57800
4	**pyochelin** $[M+H]^+$, $[M+Na]^+$	324.0602	-2.42	302	9706	22623	53181
5	**thaxtomin A** $[M+Na]^+$, $[2M+Na]^+$, $[M+K]^+$, $[M+H]^+$	438.1539	-1.93	50609	37131	2237	114
6	**desferrioxamine D1** $[M+H]^+$	602.3639	-3.83	0	9	1629	28676
7	**germicidin A** $[M+H]^+$	196.1099	-2.83	2023	7025	11790	23819
8	**geosmin** $[2M+Na]^+$	182.1670	-7.18	13655	18662	14807	11798
9	**desferrioxamine D2** $[M+Na]^+$	586.6782	-1.80	0	0	470	14193
10	**desferrioxamine F** $[M+H-2H_2O]^+$	632.3744	-4.92	0	0	29	7062
11	**desferrioxamine Et3** $[M+H-2H_2O]^+$, $[M+H]^+$	606.2860	-3.07	15	30	700	9208
12	**bottromycin A2** $[M+H]^+$, $[M+Na]^+$, $[M+K]^+$	822.4462	-1.26	0	0	250	8143
13	**desferrioxamine G** $[M+H-2H_2O]^+$	618.3588	-8.32	0	17	532	7402
14	**desferrioxamine Et1** $[M+Na]^+$	602.3275	-6.12	5	153	1820	6019
15	**turgichelin** $[2M+Na]^+$	634.3286	2.15	0	0	16	5392
16	**desferrioxamine X1** $[M+Na]^+$	572.3169	-3.16	0	41	521	2012
17	**scabichelin** $[M+Na]^+$, $[M+K]^+$	647.3602	-3.51	52	39	53	1857
18	**cyclo(L-Val-L-Pro)** $[M+H]^+$	196.1211	-4.82	672	1005	1359	1775
19	**desferrioxamine X6** $[M+H-2H_2O]^+$	612.3846	1.17	746	1755	1672	1679
20	**desferrioxamine Te2** $[M+Na]^+$	636.2611	3.20	21	99	714	1309
21	**bottromycin B2** $[M+H]^+$	808.4305	4.50	530	951	923	896
22	**desferrioxamine I2a** $[M+K]^+$	712.4007	-5.21	0	0	31	649
23	**thaxtomin B** $[M+Na]^+$	422.1590	-3.93	550	694	213	28

max > 100,000

100.000 > max > 50.000

50,000 > max > 10,000

10,000 > max > 5,000

max < 500

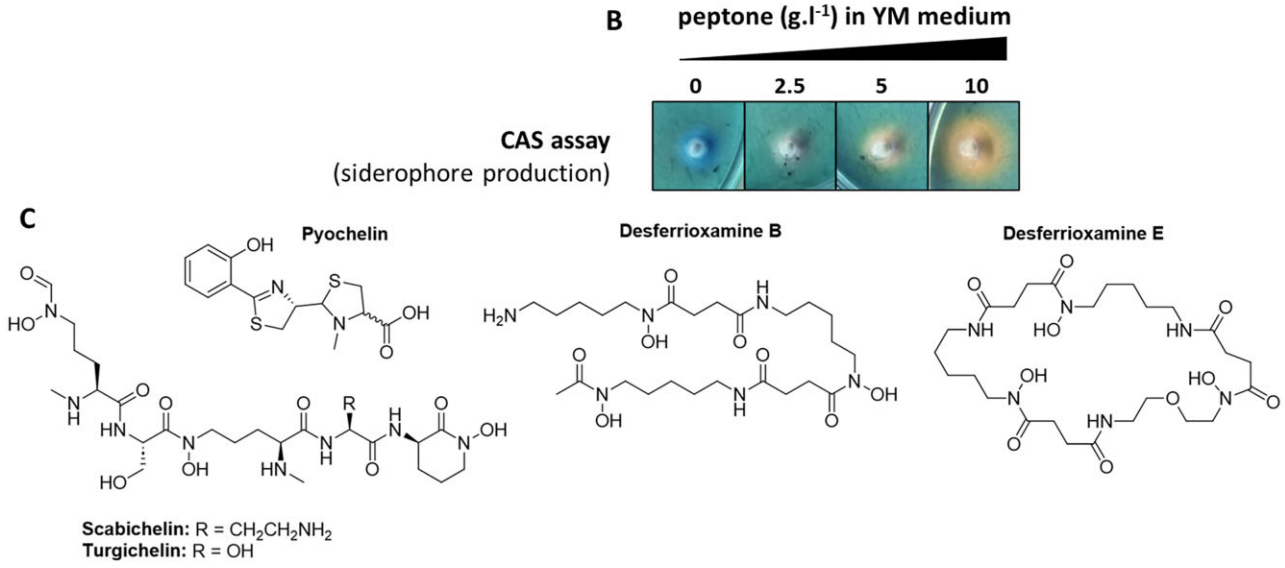

Figure 2. Peptone-mediated activation of siderophore production in *S. scabiei*. **A.** Production of known metabolites of *S. scabiei* in response to the peptone amounts in the cultivation medium. Gray-shaded line numbers indicate iron-chelating molecules. Theoretical monoisotopic masses of each metabolite are shown, together with the calculated error in ppm. Metabolite abundance values are the mean normalized abundance of three biological replicates each with two technical replicates, as calculated by Progenesis QI. The color code groups metabolites with different maximal/minimal ranges of abundance values. **B.** Chrome azurol S agar diffusion (CASAD) assay assessing the production of siderophores by *S. scabiei* according to the amount of peptone in the YM cultivation medium. **C.** The structures of four main siderophores of *S. scabiei*, DFOB (desferrioxamine B), DFOE (desferrioxamine E), pyochelin, scabichelin, and turgichelin.

restrictum NS1. The iron-associated growth restoration effect is significantly more visible when $FeCl_3$ is added to the more diluted culture extract (50% dilution) of *S. scabiei*. The fact that the growth is not fully restored confirmed the presence of other compounds with antifungal activity in the culture extract of *S. scabiei*.

The same experiments were performed with pure DFOB instead of the complex culture extracts in which multiple siderophores and other compounds are present. Figure 6D shows that adding equimolar concentrations of DFOB and $FeCl_3$ in the medium results in the loss of iron chelation signal in CAS assays confirming that all DFOB is complexed to ferric iron. The addition of DFOB to the cultivation medium drastically impairs the growth of *P. restrictum* NS1 (Fig. 6E and F). In contrast, DFOB loses its inhibitory effect when the molecule is complexed to ferric

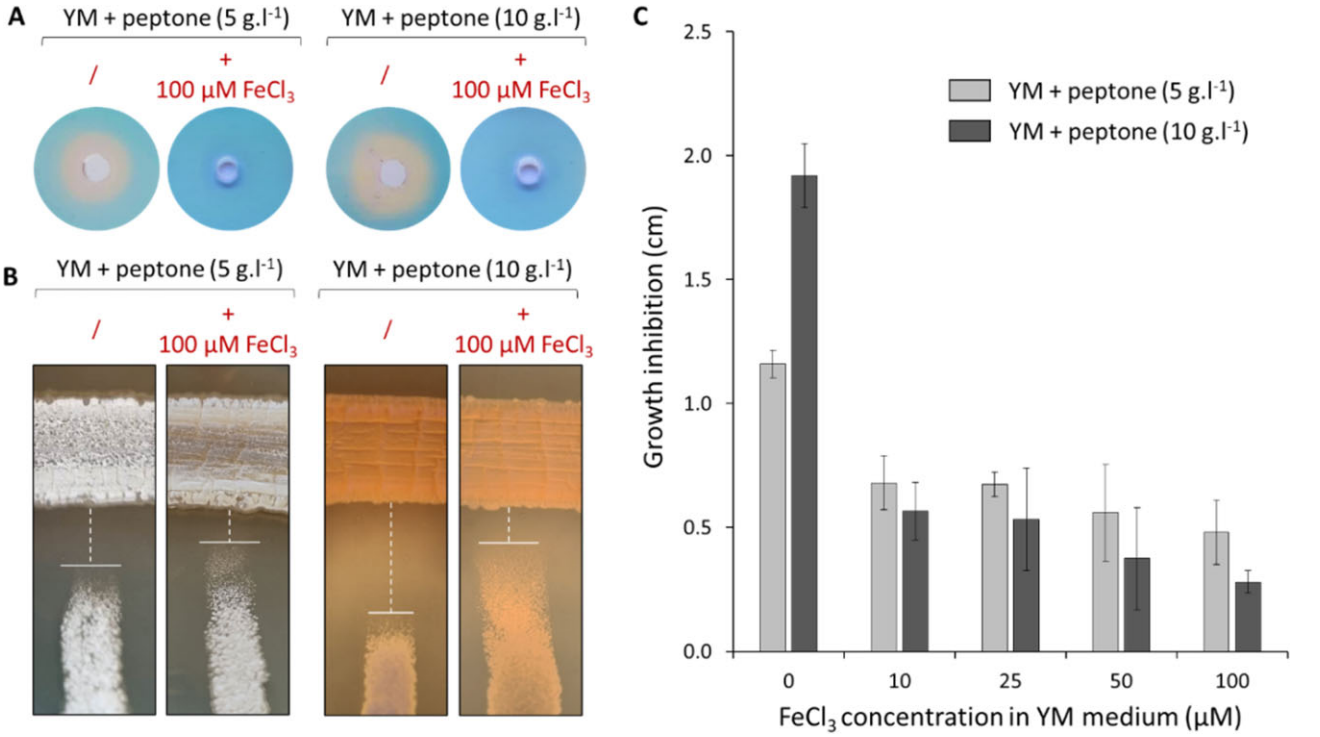

Figure 3. Effect of iron supply on siderophore production and the antifungal activity of *S. scabiei*. **A.** CAS agar diffusion assay with extracts of *S. scabiei* cultivated in YM containing either 5 or 10 $g \cdot l^{-1}$ of peptone without and with 100 µM of $FeCl_3$. **B.** Cross-streak against *P. restrictum* NS1 with *S. scabiei* cultivated in YM containing either 5 or 10 $g \cdot l^{-1}$ of peptone without and with 100 µM of $FeCl_3$. **C.** Quantification of the reduced growth inhibition of *P. restrictum* NS1 by *S. scabiei* following the addition of 10–100 µM of $FeCl_3$. Error bars represent standard deviations expressing the variability among three biological replicates for each condition.

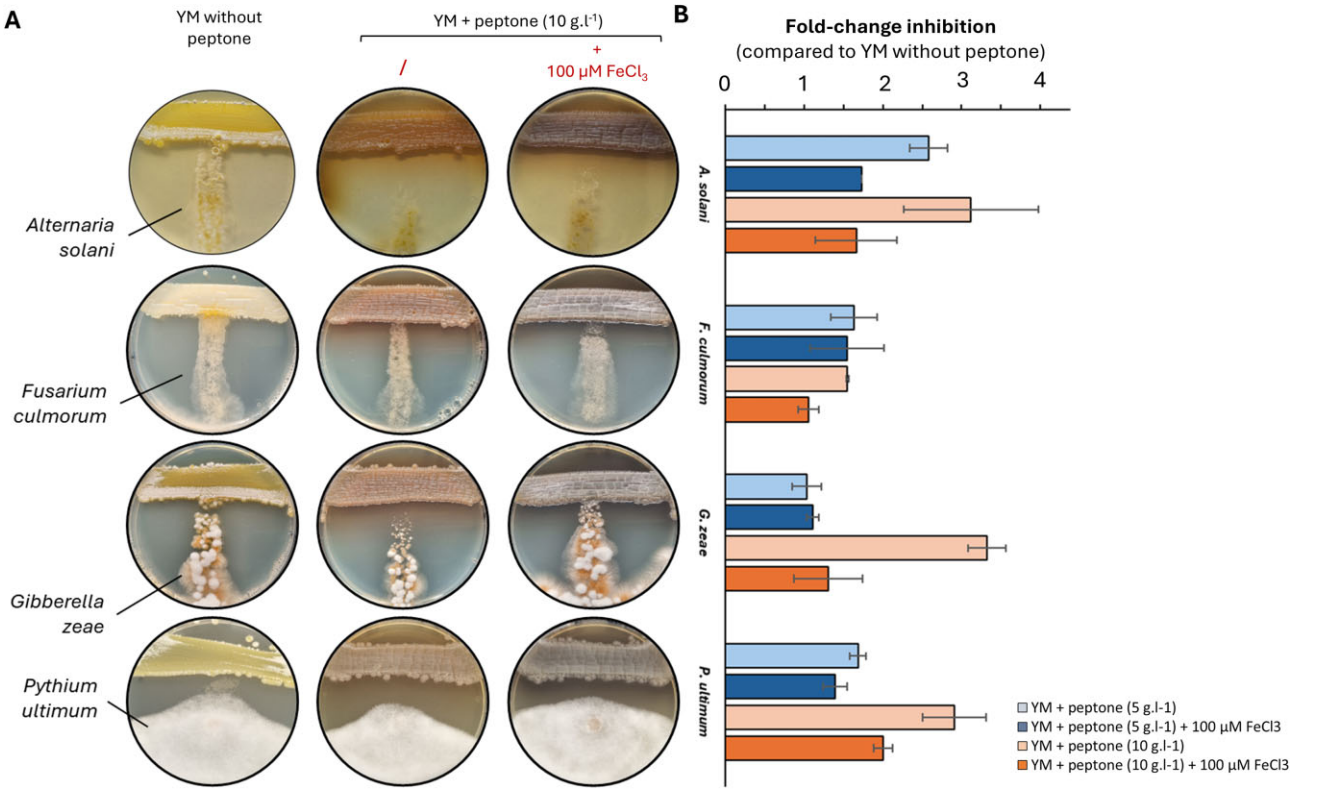

Figure 4. Contribution of the siderophore-mediated growth inhibition of plant pathogens. (**A**) Growth inhibition effects of *S. scabiei* on the YM medium supplemented with 10 g of peptone, in the presence and absence of 100 µM of $FeCl_3$ against *A. solani*, *F. culmorum*, *G. zeae*, and *P. ultimum*. (**B**) Semiquantitative evaluation of growth inhibition activity mediated by iron sequestration. The fold-change inhibition is compared to the growth inhibition measured on the YM medium without peptone.

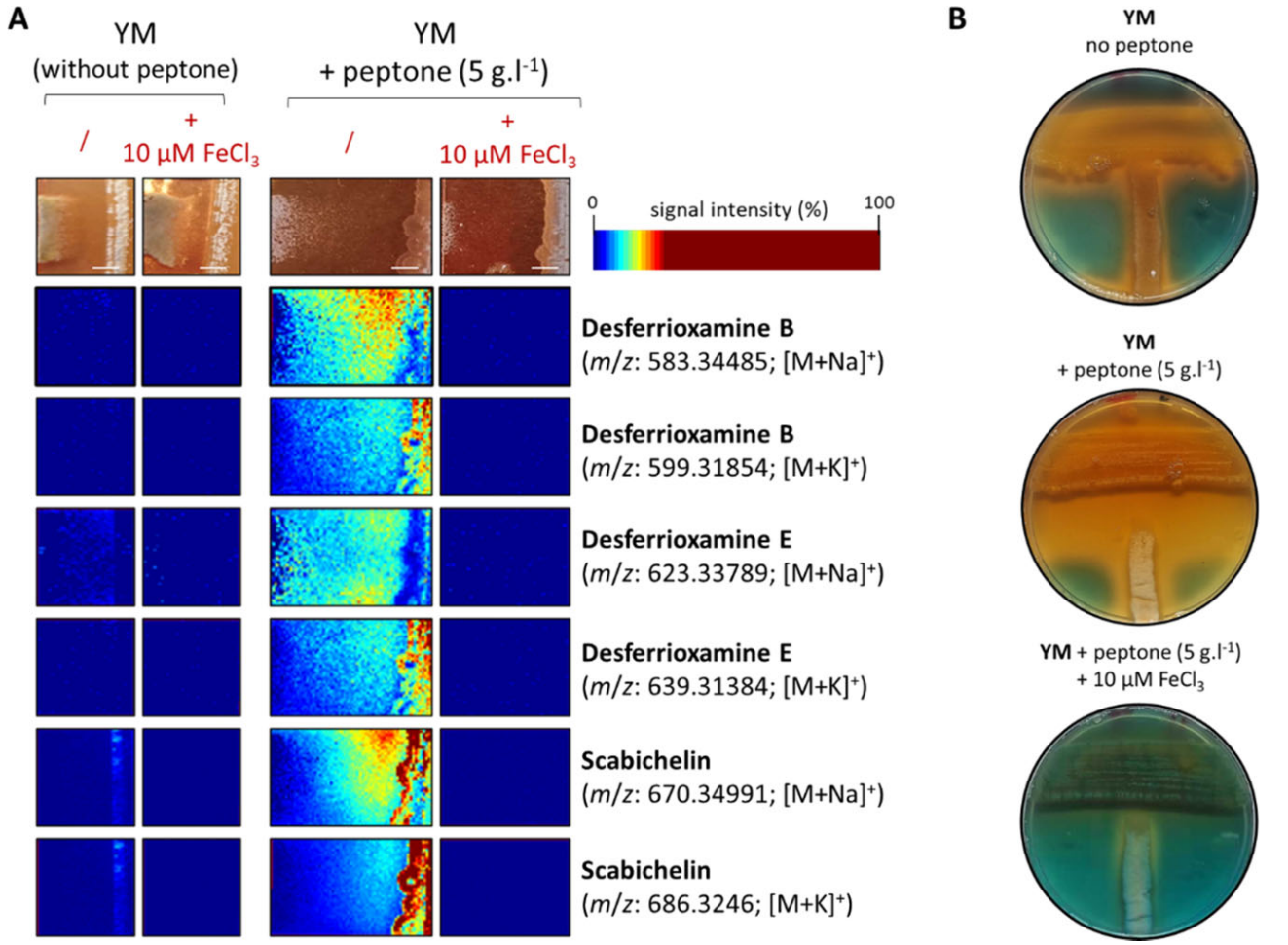

Figure 5. Mass spectrometry imaging (MSI) of antagonism between *S. scabiei* and *P. restrictum* NS1. **A**. Sodiated and potassiated adducts of desferrioxamine and scabichelin siderophores are produced when *S. scabiei* is grown in the peptone-containing YM medium and repressed upon $FeCl_3$ supply. Ion abundance is visualized using a false-color scale. Bar in top panels = 0.3 cm. **B**. Siderophore production and their contribution to the inhibition were also visualized through CAS agar overlay on cross-streak assays.

iron (Fig. 6E and F). These results confirm that the siderophores produced by *S. scabiei* can inhibit the growth of *P. restrictum* NS1 through exploitative competition for iron.

Nitrogen sources assist siderophore production

In streptomycetes, like in other bacteria, siderophore production is classically controlled by the amount of ferric iron available through repressive transcriptional regulators (DmdR1) sensing the intracellular level of ferrous iron (iron homeostasis) [29, 30]. The question remains whether the amino acids and oligopeptides present in peptone directly impact siderophore production (via their perception or their utilization), or indirectly by changing the properties of the cultivation medium. Indeed, as peptone is a rich source of nitrogen, its addition to the YM is predicted to increase the pH of the cultivation medium, which would ultimately result in decreasing the solubility—and therefore the availability—of ferric iron [31, 32], thereby possibly boosting the production of siderophores. Figure 7A shows how the addition of different quantities of peptone modifies the pH of the YM medium. At 5 $g{\cdot}l^{-1}$, peptone raises the pH of the growth medium to 8.3. The pH is not significantly more impacted with higher quantities of peptone as it reaches 8.6 at 10 and 25 $g{\cdot}l^{-1}$. However, the pH of the culture medium is not impacted at 2.5 $g{\cdot}l^{-1}$ of peptone whereas we could already observe a significant activation of siderophore production by *S. scabiei* (Fig. 7A). To further assess a possible role of the alkalinization of the medium in siderophore production, we modified the pH by adding NaOH to the YM medium, i.e. without adding nitrogen sources and therefore without boosting the nitrogen metabolism of *S. scabiei*. The alkalinization of the YM by NaOH supply did not modify the level of siderophore produced by *S. scabiei* (Fig. 7B), thereby suggesting that it is the catabolism of amino acids and oligopeptides present in peptone that would be responsible of this phenomenon.

Although the activating effect of peptone on siderophore production is drastic, peptone is not a natural source of nitrogen. It is also possible that peptides in peptone could directly chelate iron, thereby causing iron starvation and thus siderophore production. We therefore assessed whether natural organic and inorganic sources of nitrogen that cannot chelate iron such as ammonium nitrate (NH_4NO_3), sodium nitrate ($NaNO_3$), ammonium sulfate ($(NH_4)_2SO_4$), and urea (CH_4N_2O), which are commonly used as nitrogen soil fertilizers, would also trigger siderophore production in *S. scabiei*. As it can be visualized by CAS color change, all tested nitrogen sources are able to induce siderophore

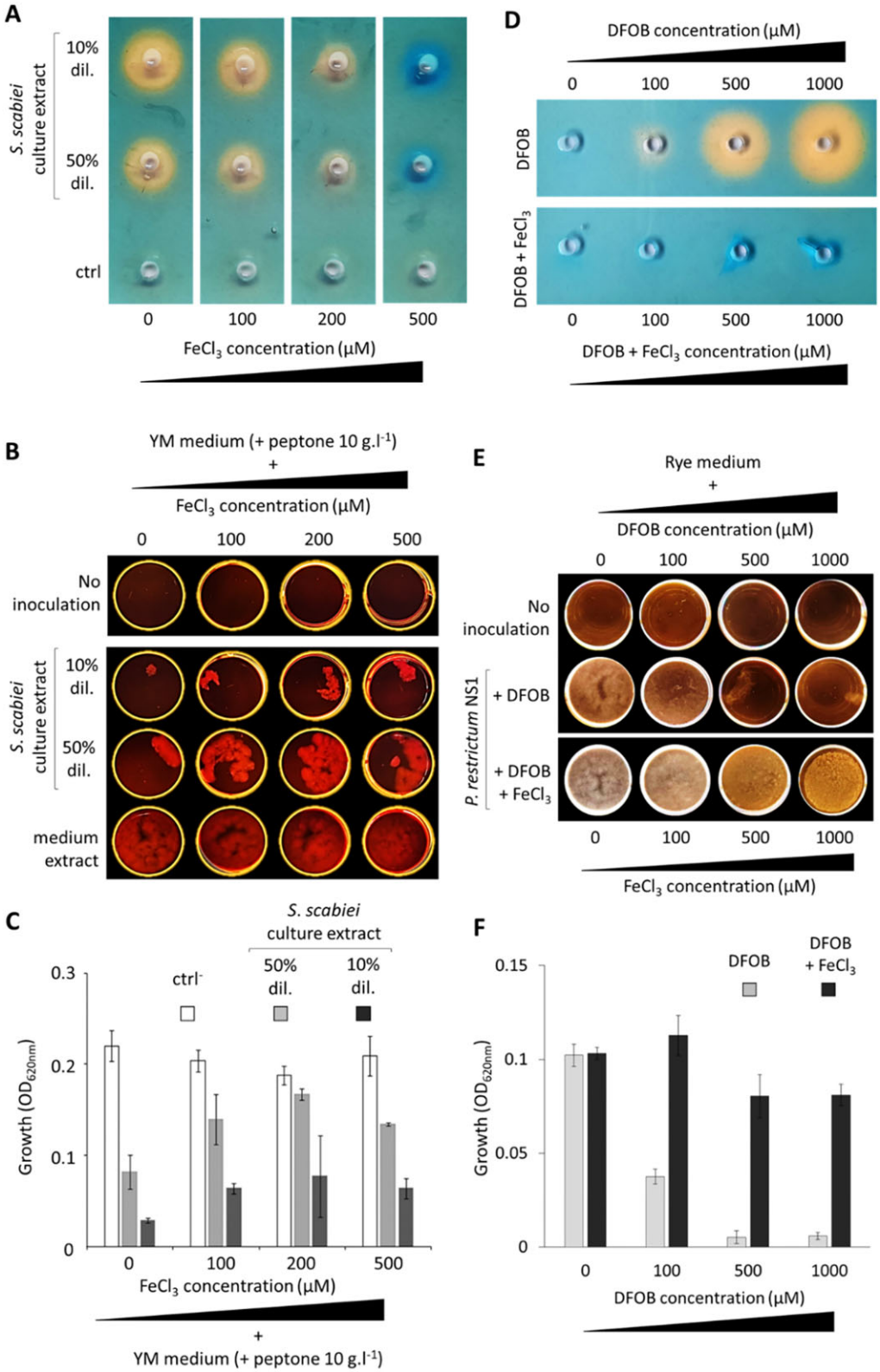

Figure 6. Siderophores of *S. scabiei* impair the growth of *P. restrictum* NS1. Top panels: Estimation of the concentration of $FeCl_3$ needed to neutralize the iron-chelating activity of two dilutions (10% and 50%) of the *S. scabiei* culture extracts (**A**), or of DFOB at different concentrations (0–1000 µM) (**D**). Middle panels: Effect of addition of iron on the growth inhibitory activity of two dilutions of the *S. scabiei* culture extracts (**B**), and of different concentrations of DFOB (**E**). Bottom panels: Quantification of B (**C**) and E (**F**). ctrl in B: Absence of the culture extract of *S. scabiei*. Values represent the mean ± SD of at least three biological replicates.

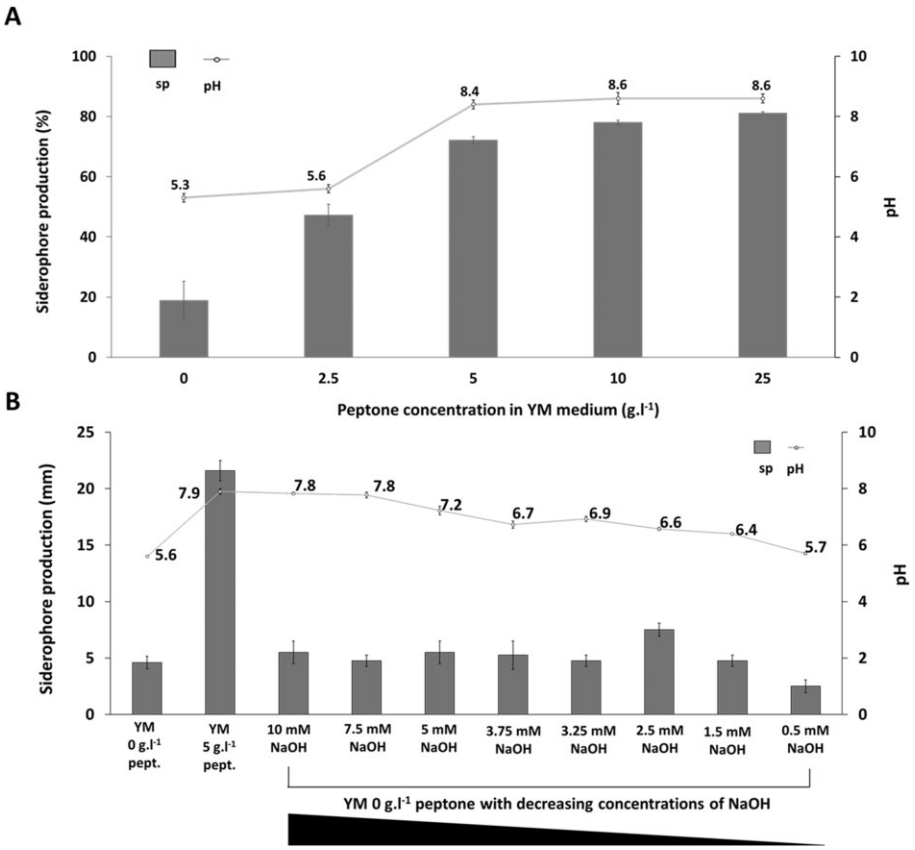

Figure 7. Influence of the pH on siderophore production by *S. scabiei*. **A.** Quantification of siderophore production by *S. scabiei* (absorbance at 630 nm, % siderophore unit) and modification of the pH at different concentration of peptone. **B.** Measurement of siderophores produced in alkalinized media (adjusted by NaOH) using CAS agar overlay (mm). Values represent the mean ± SD of four biological replicates. Note: The pH was either measured after solubilization of the agar spent (A), or the pH test strips were directly inserted into the agar (B).

production compared to the level of siderophore produced in the YM medium without additional nitrogen sources (Fig. 8). This increased production of siderophore correlates with the increased growth inhibition of the tested microorganisms (Fig. 8 and Supplementary File S4). These results suggest that nitrogen fertilizers can also drastically impact the siderophore-mediated competition for iron between soil-dwelling plant-associated microorganisms.

Conclusions

Unlike many other *Streptomyces* species, the antimicrobial potential of the model species *S. scabiei* 87-22 has been relatively underexplored, largely due to its established role as a plant pathogen. While previous research has predominantly focused on its colonization-related metabolites, our study attempted to bridge this gap by offering the first comprehensive analysis of how *S. scabiei* inhibits the growth of other microorganisms. Our results showed that next to concanamycins and volatile compounds, *S. scabiei* displays antagonistic activities through the production of siderophores that scavenge iron, making this vital nutrient less available to other microorganisms. Although siderophore-mediated iron competition has been abundantly documented, the most interesting result of our study arose from the identification of the elicitors that activate this process. Indeed, the most commonly used nitrogen fertilizers, namely nitrate (NO_3), ammonium (NH_4), and urea (CH_4N_2O), stimulate siderophore production. We excluded here the possibility that the observed effect would be mediated by alkalinization of the medium as increasing the pH without providing additional nitrogen sources did not induce siderophore production. Another possible explanation for nitrogen induction of siderophore production could be the consequence of increasing the source of amino acids, thereby providing more building blocks for siderophore biosynthesis. The later scenario is also supported by the fact that gene clusters involved in the biosynthesis of peptide-based secondary metabolites (such as siderophores) sometimes also contain genes involved in amino acid biosynthesis in order to increase the pool of precursor molecules independently of primary metabolism. However, this hypothesis cannot explain why nitrogen sources not used as building blocks of siderophore biosynthesis, such as sodium nitrate, ammonium, and urea, also induce siderophore production.

As siderophore biosynthesis is commonplace in streptomycetes, *S. scabiei* is unlikely to be the only player in siderophore-mediated competition for iron in the rhizosphere. Our findings suggest that nitrogen sources in fertilizers could alter microbial dynamics by enhancing siderophore production across various microorganisms, thereby intensifying the social interactions driven by siderophores (altruistic cooperation, mutually beneficial cooperation, cheating, and competition [33]), hence impacting the overall microbial balance. The prevalence of this phenomenon and the molecular mechanisms underlying nitrogen metabolism-mediated control of siderophore

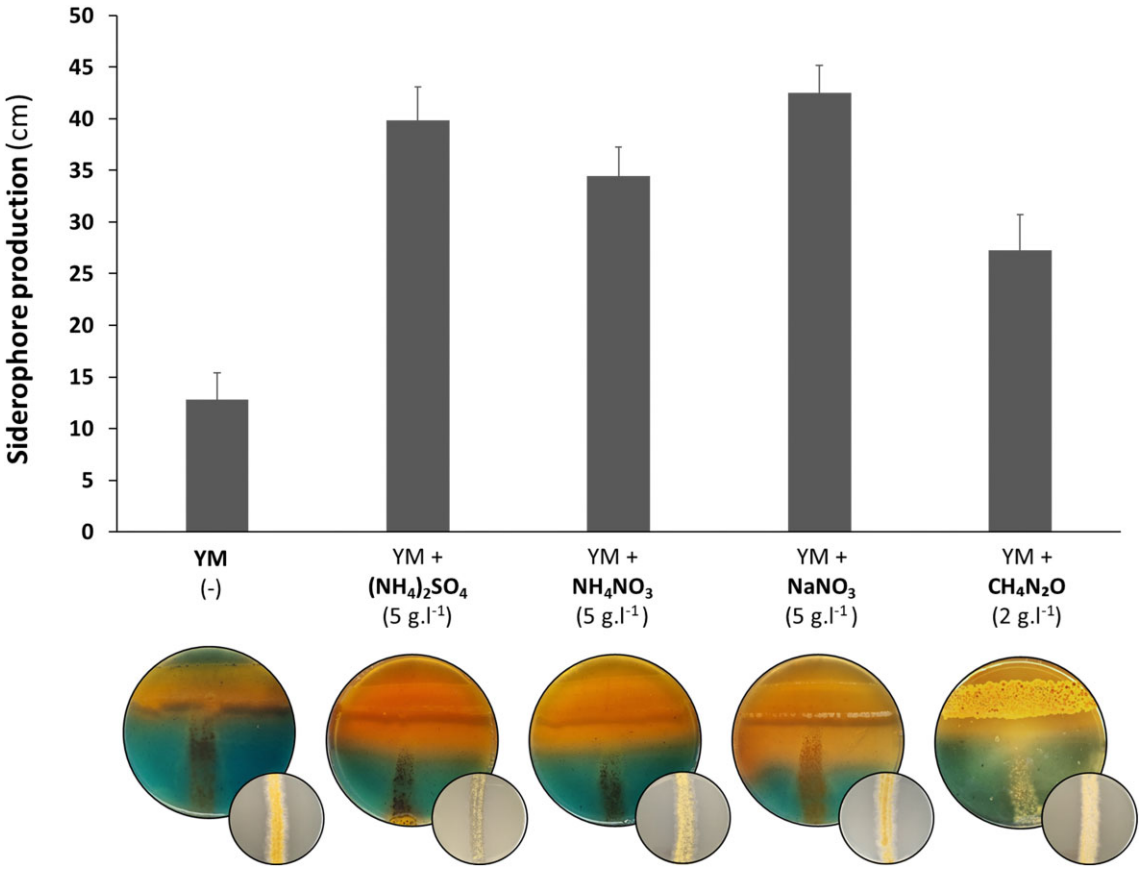

Figure 8. Effect of nitrogen fertilizers on siderophore production by *S. scabiei*. Siderophore production by *S. scabiei* was quantified on media supplemented with various nitrogen sources: ammonium sulfate ($(NH_4)_2SO_4$), ammonium nitrate (NH_4NO_3), sodium nitrate ($NaNO_3$), and urea (CH_4N_2O). Data were obtained using the CASAD assay, with values expressed as the mean ± SD from independent biological replicates. Combined monitoring of siderophore production and growth inhibition is visualized on cross-streak assays against *A. solani*. Insets in the bottom right corner of each cross-streaked plate display the growth of *A. solani* on the control plate without *S. scabiei*.

production certainly merit further investigation. Such research could advance our comprehension of microbial interactions in the rhizosphere and potentially lead to the development of novel strategies for microbial management and improved crop protection.

Acknowledgments

This research was supported by the University of Liège ('Action de Recherche Concertée') and the Fund for Scientific Research (F.R.S.—FNRS) through CDR, PDR, FRIA, and Aspirant grants. S.R. and M.O. are senior research associate and Research Director at the F.R.S.-FNRS, respectively.

Author contributions

N.S., Y.K., B.D., D.T., A.R., L.R., and S.R.: conceptualization and design of the research. N.S., Y.K., L.B., R.D., L.R., B.D., and P.B.: performance of experimental work. N.S., Y.K., L.B., R.D., L.R., P.B., L.Q., M.H., M.O., and S.R.: interpretation of results. N.S., Y.K., L.R., P.B., and S.R.: writing of the main manuscript. B.D., P.B., L.Q., M.H., M.O.: revision of the manuscript. L.Q., M.H., M.O., and S.R.: research fundings: All authors have given approval to the final version of the manuscript.

Supplementary data

Supplementary data are available at *Metallomics* online.

Conflict of interest

The authors declare that the research was conducted in the absence of any commercial or financial relationships that could be construed as a potential conflict of interest.

Funding

The work of N.S. was supported by a FRIA grant (FRIA 1.E.116.21), a PDR grant to Y.K. (T.0195.23-PDR), and an Aspirant grant from the FNRS for B.D. (1.A618.18). S.R.'s work is also supported by a 'Crédit De Recherche FNRS grant' (J.0158.21-CDR), by a 'Projet De Recherche FNRS grant' (T.0195.23-PDR), and by an 'Action de Recherche Concertée' grant (Mind Project, grant R.CFRA-3306) from the University of Liège.

Data availability

The data underlying this article are available in the article and in its online supplementary material. The raw data associated with mass spectrometry imaging analyzes will be shared on reasonable request to the corresponding author.

References

1. Treseder KK. Ecological strategies of microbes: thinking outside the triangle. *J Ecol* 2023;**111**:1832–43. https://doi.org/10.1111/1365-2745.14115
2. Chater KF, Biró S, Lee KJ *et al.* The complex extracellular biology of *streptomyces*. *FEMS Microbiol Rev* 2010;**34**:171–98. https://doi.org/10.1111/j.1574-6976.2009.00206.x
3. Chater KF, Losick R. Mycelial life style of *Streptomyces coelicolor* A3(2) and its relatives In: Shapiro JA & Dworkin M (eds.), *Bacteria as Multicellular Organisms*. New York: Oxford University Press. 1997, 149182.
4. Treseder KK, Lennon JT. Fungal traits that drive ecosystem dynamics on land. *Microbiol Mol Biol Rev* 2015;**79**:243–62. https://doi.org/10.1128/MMBR.00001-15
5. Lewin GR, Carlos C, Chevrette MG *et al.* Evolution and ecology of actinobacteria and their bioenergy applications. *Annu Rev Microbiol* 2016;**70**:235–54. https://doi.org/10.1146/annurev-micro-102215-095748
6. Klein DA, Paschke MW. Filamentous fungi: the indeterminate lifestyle and microbial ecology. *Microb Ecol* 2004;**47**:224–35. https://doi.org/10.1007/s00248-003-1037-4
7. Raines DJ, Moroz OV, Blagova EV *et al.* Bacteria in an intense competition for iron: key component of the *Campylobacter jejuni* iron uptake system scavenges enterobactin hydrolysis product. *Proc Natl Acad Sci USA* 2016;**113**:5850–5. https://doi.org/10.1073/pnas.1520829113
8. Jarmusch SA, Lagos-Susaeta D, Diab E *et al.* Iron-meditated fungal starvation by lupine rhizosphere-associated and extremotolerant *Streptomyces* sp. S29 desferrioxamine production. *Mol Omics* 2021;**17**:95–107. https://doi.org/10.1039/D0MO00084A
9. Gu S, Wei Z, Shao Z *et al.* Competition for iron drives phytopathogen control by natural rhizosphere microbiomes. *Nat Microbiol* 2020;**5**:1002–10. https://doi.org/10.1038/s41564-020-0719-8
10. Bignell DRD, Huguet-Tapia JC, Joshi MV *et al.* What does it take to be a plant pathogen: genomic insights from streptomyces species. *Antonie Van Leeuwenhoek* 2010;**98**:179–94. https://doi.org/10.1007/s10482-010-9429-1
11. Deflandre B, Stulanovic N, Planckaert S *et al.* The virulome of *Streptomyces scabiei* in response to cello-oligosaccharide elicitors. *Microb Genom* 2022;**8**:000760.
12. Liu J, Nothias L-F, Dorrestein PC *et al.* Genomic and metabolomic analysis of the potato common scab pathogen *Streptomyces scabiei*. *ACS Omega* 2021;**6**:11474–87. https://doi.org/10.1021/acsomega.1c00526
13. Kerff F, Jourdan S, Francis IM *et al.* Common scab disease: structural basis of elicitor recognition in pathogenic *Streptomyces* species. *Microbiol Spectr* 2023;**11**:e0197523.
14. Han W-C, Lee J-Y, Park D-H *et al.* Isolation and antifungal and antioomycete activity of *Streptomyces scabiei* strain PK-A41, the causal agent of common scab disease. *Plant Pathol J* 2004;**20**:115–26. https://doi.org/10.5423/PPJ.2004.20.2.115
15. Loria R, Bukhalid R, Creath R *et al.* Differential production of thaxtomins by pathogenic *streptomyces* species in vitro. *Phytopathology* 1995;**85**:537–41. https://doi.org/10.1094/Phyto-85-537
16. Kieser T, Bibb MJ, Buttner MJ *et al. Practical Streptomyces Genetics*. Colney, Norwich, England: John Innes Foundation, 2000.
17. Shirling EB, Gottlieb D. Methods for characterization of streptomyces species 1. *Int J Syst Evol Microbiol* 1966;**16**:313–40. https://doi.org/10.1099/00207713-16-3-313
18. Caten C, Jinks J. Spontaneous variability of single isolates of *Phytophthora infestans*. I. Cultural variation. *Can J Bot* 1968;**46**:329–48. https://cdnsciencepub.com/doi/abs/10.1139/b68-055?journalCode=cjb1 (17 September 2023, date last accessed).
19. Adam D, Maciejewska M, Naômé A *et al.* Isolation, characterization, and antibacterial activity of hard-to-culture actinobacteria from cave moonmilk deposits. *Antibiotics (Basel)* 2018;**7**:28. https://doi.org/10.3390/antibiotics7020028
20. Maciejewska M, Adam D, Martinet L *et al.* A phenotypic and genotypic analysis of the antimicrobial potential of cultivable *streptomyces* isolated from cave moonmilk deposits. *Front Microbiol* 2016;**7**:1455. https://doi.org/10.3389/fmicb.2016.01455
21. Schwyn B, Neilands JB. Universal chemical assay for the detection and determination of siderophores. *Anal Biochem* 1987;**160**:47–56. https://doi.org/10.1016/0003-2697(87)90612-9
22. Shin SH, Lim Y, Lee SE *et al.* CAS agar diffusion assay for the measurement of siderophores in biological fluids. *J Microbiol Methods* 2001;**44**:89–95. https://doi.org/10.1016/S0167-7012(00)00229-3
23. Craig M, Lambert S, Jourdan S *et al.* Unsuspected control of siderophore production by N-acetylglucosamine in streptomycetes. *Environ Microbiol Rep* 2012;**4**:512–21. https://doi.org/10.1111/j.1758-2229.2012.00354.x
24. Lambert S, Traxler MF, Craig M *et al.* Altered desferrioxamine-mediated iron utilization is a common trait of bald mutants of *Streptomyces coelicolor*. *Metallomics* 2014;**6**:1390–9. https://doi.org/10.1039/C4MT00068D
25. Arora NK, Verma M. Modified microplate method for rapid and efficient estimation of siderophore produced by bacteria. *3 Biotech* 2017;**7**:381. https://doi.org/10.1007/s13205-017-1008-y
26. Sinclair E, Trivedi DK, Sarkar D *et al.* Metabolomics of sebum reveals lipid dysregulation in Parkinson's disease. *Nat Commun* 2021;**12**:1592. https://doi.org/10.1038/s41467-021-21669-4
27. Sun Y, Cheng G, Du L *et al.* Chuanzhitongluo capsule ameliorates microcirculatory dysfunction in rats: efficacy evaluation and metabolic profiles. *Front Pharmacol* 2022;**13**:1011333. https://doi.org/10.3389/fphar.2022.1011333
28. Burguet P, La Rocca R, Kune C *et al.* Exploiting differential signal filtering (DSF) and image structure filtering (ISF) methods for untargeted mass spectrometry imaging of bacterial metabolites. *J Am Soc Mass Spectrom* 2024;**35**:1743–55. https://doi.org/10.1021/jasms.4c00129
29. Flores FJ, Martín JF. Iron-regulatory proteins DmdR1 and DmdR2 of *streptomyces coelicolor* form two different DNA-protein complexes with iron boxes. *Biochem J* 2004;**380**:497–503. https://doi.org/10.1042/bj20031945
30. Tunca S, Barreiro C, Sola-Landa A *et al.* Transcriptional regulation of the desferrioxamine gene cluster of *Streptomyces coelicolor* is mediated by binding of DmdR1 to an iron box in the promoter of the *desA* gene. *FEBS J* 2007;**274**:1110–22. https://doi.org/10.1111/j.1742-4658.2007.05662.x
31. Johnson DB, Kanao T, Hedrich S. Redox transformations of iron at extremely low pH: fundamental and applied aspects. *Front Microbiol* 2012;**3**:96. https://doi.org/10.3389/fmicb.2012.00096
32. Monhemius A. Precipitation diagrams for metal hydroxydes, sulphides, arsenates and phosphates. *Trans Inst Min Metall* 1977;**86**:C202–6.
33. Kramer J, Özkaya Ö, Kümmerli R. Bacterial siderophores in community and host interactions. *Nat Rev Micro* 2020;**18**:152–63. https://doi.org/10.1038/s41579-019-0284-4

Received: August 19, 2024. **Accepted:** October 22, 2024
© The Author(s) 2024. Published by Oxford University Press. All rights reserved. For permissions, please e-mail: journals.permissions@oup.com